American Mineralogist, Volume 106, pages 1580–1585, 2021

The suppression of lone-pair stereoactivity in $[Cu^{+}(As^{3+}O_3)_4]$ clusters in dixenite: A tribute to Paul B. Moore

Frank C. Hawthorne[1] and John M. Hughes[2,*]

[1]Department of Geological Sciences, University of Manitoba, Winnipeg, Manitoba, R3T 2N2, Canada
[2]Department of Geology, University of Vermont, Burlington, Vermont 05405, U.S.A.

Abstract

The crystal structure of dixenite, ideally $Cu^{+}Fe^{3+}Mn^{2+}_{14}(As^{5+}O_4)(As^{3+}O_3)_5(SiO_4)_2(OH)_6$, from Långban, Sweden, was refined to an R_1-index of 1.58%, and the structure proposed by Araki and Moore (1981) was confirmed and details elucidated. The structure, crystallizing in space group $R3$ with a = 8.2204(3) and c = 37.485(3) Å, consists of layers of $(Mn^{2+},Fe^{3+})(O,OH)_6$ octahedra linked by $(As^{5+}O_4)$ and (SiO_4) tetrahedra, $(As^{3+}O_3)$ trigonal pyramids, and $(Cu^{+}As^{3+}_4)$ tetrahedra. There are five distinct layers in the repeat unit of the cell, four of which are very similar to the layers in mcgovernite. An unusual aspect of one of the trimers of octahedra is that there is a triangular-prismatic hole through the center of the cluster. The $(Cu^{+}As^{3+}_4)$ tetrahedra are parts of larger clusters: $[Cu^{+}(As^{3+}O_3)_4]$ in which four $(As^{3+}O_3)$ groups link to a central Cu^{+} that occupies the positions normally taken by the stereoactive lone-pairs of electrons that generally characterize As^{3+} in triangular-pyramidal coordination by O. Thus, the stereoactive lone-pair behavior that is characteristic of $(As^{3+}O_3)$ trigonal pyramids is suppressed by the coordination of Cu^{+} by four As^{3+} ions.

Keywords: Dixenite, crystal structure, lone-pair electrons, Paul B. Moore

Introduction

Paul Brian Moore (1940–2019) was one of the giants of mineralogy, and his legacy lives in the numerous papers he published in his distinguished career. His contributions to mineralogy were celebrated in a recent memorial (Hawthorne et al. 2019) that stated that he was the greatest mineralogist of the 20th century. Professor Moore and his colleagues solved numerous complex structures in an age before (usually) routine solution of crystal structures using direct methods was possible, stretching the limits of equipment and computational resources of that time. As noted in his memorial, even in retirement, Paul never stopped thinking about problems involving crystal structures. In addition to being involved with new atomic arrangements, he urged colleagues to re-examine some of his earlier solutions that were done with the diffraction equipment of an earlier day. One of those structures was that of dixenite, which was a frequent source of conversations with his colleagues. At the time of his death, Professor Moore was urging both of us to re-examine the dixenite structure, and we are pleased to offer the results of that work here.

Dixenite, ideally $Cu^{+}Fe^{3+}Mn^{2+}_{14}(As^{5+}O_4)(As^{3+}O_3)_5(SiO_4)_2(OH)_6$, is of considerable interest because it has a novel metallic cluster, ideally $(Cu^{+}As^{3+}_4)$, embedded in an oxide environment (Araki and Moore 1981), an atomic arrangement that had not been observed previously in any structure. At the same time, Moore and Araki (1979) found another metallic cluster, $(Mn^{+}As^{3+}_6)$, embedded in an oxide environment in magnussonite, ideally $Mn^{2+}_{18}[Mn^{+}As^{3+}_6O_{18}]_2Cl_2$. As far as we are aware, these are the only examples of such clusters found in minerals, and Paul B. Moore (personal communication) was keen to see confirmation of these findings by more accurate modern instrumentation. Moreover, both these minerals occur only in the (Fe-Mn)-oxide ore deposits at Långban, Sweden (Moore 1970; Holtstam and Langhof 1999; Lundström 1999; Bollmark 1999; Nysten et al. 1999), and we have a long-term interest in the basic Mn-arsenate-silicate minerals from this locality (Hawthorne 2018; Hawthorne et al. 2013; Cooper and Hawthorne 1999, 2012).

Sample provenance

Both samples examined here are from Långban. One sample was obtained from the U.S. National Museum of Natural History (C4440, provided to Paul B. Moore) and the other from the late Mark Feingloss, a well-known mineral collector from Duke University. The structural results are virtually identical, and we present only one refinement here.

Crystal structure

Data collection and refinement

A crystal fragment from NMNH C4440 was mounted on a Bruker Apex CCD diffractometer equipped with graphite-monochromated Mo$K\alpha$ radiation. Refined cell parameters and other crystal data are listed in the deposited CIF[1]. Redundant data were collected for a sphere of reciprocal space and were integrated and corrected for Lorentz and polarization factors and absorption using the Bruker program SaintPlus.

The atomic arrangement was solved independently of that given by Araki and Moore (1981), and hydrogen positions were located using difference-Fourier maps. The structure is in close agreement with that of Araki and Moore (1981); we have retained their original atom nomenclature in this paper. Refine-

* E-mail: jmhughes@uvm.edu

0003-004X/21/0010–1580$05.00/DOI: https://doi.org/10.2138/am-2021-7719

ment was done with anisotropic-displacement parameters for all atoms except H. Table 1 lists the refined atom parameters, Table 2 lists selected interatomic distances, and Table 3 gives the bond-valence table (v.u.; valence units) calculated with the parameters of Gagné and Hawthorne (2015). A CIF[1] has been deposited, which contains further details of crystal data and structure refinement.

Site populations

The atomic arrangement is virtually identical to that given by Araki and Moore (1981), although of much greater precision. There are three As sites with associated coordinations, bond lengths, and angles characteristic of As^{3+}. Each As^{3+} is coordinated by three O^{2-} ions at distances from 1.726–1.776 Å, in the range of $^{[3]}As^{3+}$-O distances shown by inorganic crystal-structures: 1.671–1.845 Å (Gagné and Hawthorne 2018) and close to the grand mean $^{[3]}As^{3+}$-O distance of 1.776 Å. There are three T sites that have site-scattering values between Si and As; each site is coordinated by a tetrahedral arrangement of O atoms and have T-O distances (Table 2) that are intermediate between those expected for $^{[4]}$Si-O and $^{[4]}As^{5+}$-O in oxide and oxysalt structures (Gagné and Hawthorne 2018). There are six

TABLE 1. Atom coordinates and equivalent isotropic atom-displacement parameters (Å²) for dixenite

Atom	x/a	y/b	z/c	U(eq)	Occ.
As1	1/3	2/3	0.93013(3)	0.00961(13)	$As_{1.00}$
As2	2/3	1/3	0.74936(3)	0.00925(13)	$As_{1.00}$
As3	0.91124(5)	0.62586(6)	0.68425(3)	0.01006(9)	$As_{1.00}$
T1SI	1/3	2/3	0.81217(5)	0.0065(5)	$Si_{0.946(7)}As_{0.054}$
T2AS	0	0	0.85378(4)	0.0079(3)	$Si_{0.458}As_{0.542(7)}$
T3AS	2/3	1/3	0.88640(3)	0.0073(3)	$Si_{0.275}As_{0.725(7)}$
M1	0	0	0	0.01162(19)	$Mn_{1.00}$
M2	2/3	1/3	0.99435(5)	0.0177(4)	$Mn_{0.937(5)}$
M2A	2/3	1/3	0.9635(7)	0.030(6)	$Cu_{0.063}$
M3	0	0	0.74267(4)	0.0091(3)	$Fe_{0.943(6)}$
M4	0.95815(9)	0.73646(9)	0.93256(3)	0.01243(13)	$Mn_{1.00}$
M5	0.58214(9)	0.66184(10)	0.87042(3)	0.01397(13)	$Mn_{1.00}$
M6	0.89166(9)	0.60100(9)	0.80761(3)	0.01194(13)	$Mn_{1.00}$
M7	0.57710(9)	0.68485(9)	0.73874(3)	0.01028(12)	$Mn_{1.00}$
Cu1	2/3	1/3	0.68694(5)	0.0104(5)	$Cu_{0.663(7)}$
Cu2	1/3	2/3	0.99682(19)	0.0162(19)	$Cu_{0.190(6)}$
O1	0	0	0.89791(15)	0.0155(10)	$O_{1.00}$
O2	1/3	2/3	0.17418(14)	0.0153(10)	$O_{1.00}$
O3	1/3	2/3	0.76863(13)	0.0091(8)	$O_{1.00}$
O4	0.9104(5)	0.5555(4)	0.97864(9)	0.0162(6)	$O_{1.00}$
O5	0.5305(4)	0.8340(4)	0.90522(8)	0.0115(5)	$O_{1.00}$
O6	0.7168(4)	0.5446(4)	0.90093(9)	0.0130(6)	$O_{1.00}$
O7	0.8341(4)	0.7922(4)	0.83826(9)	0.0105(5)	$O_{1.00}$
O8	0.4810(4)	0.8724(4)	0.82948(8)	0.0125(5)	$O_{1.00}$
O9	0.6318(4)	0.4991(4)	0.77256(8)	0.0105(5)	$O_{1.00}$
O10	0.8531(4)	0.7722(4)	0.70923(9)	0.0129(5)	$O_{1.00}$
O11	0.5380(4)	0.8815(4)	0.70443(8)	0.0108(5)	$O_{1.00}$
OH1	0.7869(4)	0.8217(4)	0.96239(9)	0.0125(5)	$O_{1.00}$
H1	0.697(8)	0.719(8)	0.9679(15)	0.008(12)	$H_{1.00}$
OH2	0.7648(4)	0.9183(4)	0.77301(9)	0.0116(5)	$O_{1.00}$
H2	0.758(11)	0.852(11)	0.793(2)	0.04(2)	$H_{1.00}$

Note: U(eq) is defined as one third of the trace of the orthogonalized U_{ij} tensor.

TABLE 2. Selected bond distances (Å) in dixenite

	Distance		Distance		Distance
As1-O5(×3)	1.7782(31)	As2-O9(×3)	1.7567(29)	As3-O4	1.7300(32)
Mean	1.778	Mean	1.757	-O11	1.7634(28)
				-O10	1.7684(30)
				Mean	1.754
T1SI-O3	1.6320(53)	T2AS-O1	1.6544(56)	T3AS-O6(×3)	1.6634(30)
-O8(×3)	1.6438(32)	-O7(×3)	1.6694(28)	-O2	1.7076(54)
Mean	1.641	Mean	1.666	Mean	1.674
M1-OH1(×3)	2.1533(33)	M2-*M2A*	*1.1580(250)*	M2A-*M2*	*1.1580(250)*
-O11(×3)	2.2318(30)	-O4(×3)	2.0094(32)	-O4(×3)	2.0036(78)
Mean	2.193	-O10(×3)	2.4437(35)	Mean	2.004
		Mean	2.227		
M3-OH2(×3)	2.0455(31)	M4-O5	2.1537(30)	M5-O8	2.0859(30)
-O10(×3)	2.0675(31)	-OH1	2.1584(32)	-O5	2.1177(30)
Mean	2.057	-O6	2.1679(31)	-O6	2.1282(31)
		-OH1	2.1701(31)	-O7	2.1614(31)
		-O4	2.1832(32)	-O5	2.4136(32)
		-O1	2.3985(30)	-O8	2.7354(32)
		Mean	2.205	Mean	2.274
M6-O8	2.0777(31)	M7-OH2	2.1803(30)	Cu1-*Cu2*	*0.8789(67)*
-O7	2.1815(30)	-O9	2.1973(29)	-As3(×3)	2.2361(4)
-OH2	2.2454(32)	-O11	2.2112(29)	-As2	2.3400(18)
-O9	2.2460(30)	-O3	2.2347(25)	Mean	2.262
-O9′	2.2805(30)	-O11	2.2762(30)		
-O2	2.3968(29)	-O10	2.2928(31)		
Mean	2.238	Mean	2.232		
Cu2-*Cu1*	*0.8789(67)*				
-As3(×3)	2.3654(24)				
-As1	2.5001(72)				
Mean	2.399				

Note: Bond distances in italics are to second cation occupant in split site and are not included in mean.

TABLE 3. Bond-valence (v.u.) table for dixenite

	M(1)	M(2)	M(3)	M(4)	M(5)	M(6)	M(7)	T(1)	T(2)	T(3)	As(1)	As(2)	As(3)	Σ
O(1)				$0.21^{x3\rightarrow}$					1.17					1.80
O(2)						$0.21^{x3\rightarrow}$				1.08				1.71
O(3)							$0.31^{x3\rightarrow}$	1.01						1.94
O(4)		$0.52^{x3\downarrow}$		0.34									1.11	1.97
O(5)				0.37	0.40						$0.99^{x3\downarrow}$			1.96
					0.20									
O(6)				0.36	0.39					$1.22^{x3\downarrow}$				1.97
O(7)					0.36	0.35			$1.12^{x3\downarrow}$					1.83
O(8)					0.44	0.45		$0.98^{x3\downarrow}$						1.96
					0.09									
O(9)						0.30	0.33					$1.04^{x3\downarrow}$		1.94
						0.27								
O(10)		$0.18^{x3\downarrow}$	$0.43^{x3\downarrow}$				0.27						1.01	1.89
O(11)	$0.31^{x3\downarrow}$						0.32						1.03	1.94
							0.28							
OH(1)	$0.37^{x3\downarrow}$			0.37										1.10
				0.36										
OH(2)			$0.46^{x3\downarrow}$			0.30	0.35							1.11
Σ	2.04	2.10	2.67	2.01	1.88	1.88	1.86	3.95	4.53	4.74	2.97	3.12	3.15	
	2	3	3	2	2	2	2	4.05	4.54	4.72	3	3	3	

M sites that have site-scattering values characteristic of Mn and Fe and that are octahedrally coordinated by O atoms. The observed interatomic distances (Table 2) indicate that six of these sites are occupied by Mn^{2+} with minor Fe^{2+}. The site scattering at the M3 site indicates that this site is occupied by a transition metal. The <M3-O> bond length is 2.057 Å, significantly longer than the grand <Fe^{3+}-O> distance of 2.015 Å reported by Gagné and Hawthorne (2020) for oxide and oxysalt structures. Thus, in addition to Fe^{3+}, M3 must be occupied partly by Fe^{2+} and/or Mn^{2+}, in accord with the incident bond-valence sum at M3 of 2.67 v.u. (Table 3). Polyhedra are labeled by the identity of the ion/atom at the central site: thus, the coordination octahedron of Mn^{2+} at the M1 site, $Mn^{2+}O_6$, is denoted as the M1 octahedron. The bond valences incident at the O anions (Table 3) show that OH1 and OH2 are hydroxyl groups and the remaining anions are O^{2-}. The site-scattering values and mean bond lengths are in accord with the formula $Cu^{+}Fe^{3+}Mn^{2+}_{14}(As^{5+}O_4)(As^{3+}O_3)_5(SiO_4)_2(OH)_6$ assigned by Araki and Moore (1981).

Bond topology

The dixenite structure contains 15 layers of approximately close-packed polyhedra that comprise one translation along **c**. In space group *R*3, five symmetrically and bond-topologically distinct layers are stacked orthogonal to the **c**-axis to give the ~37.5 Å repeat in the **c** direction. The five distinct layers of cation-centered polyhedra are labeled m = 0–4 in Figure 1, and these layers are shown in plan in Figure 2, where they are compared with similar layers in the crystal structure of mcgovernite (Hawthorne 2018).

At m = 0 (Fig. 2a), the layer consists of M5 octahedra containing Mn^{2+} and two distinct tetrahedra, T2As and T3As, that contain As^{5+} and Si with As^{5+} dominant at both T sites (Table 2). The M5 octahedron shows a large dispersion of bond lengths: 2.086–2.735 Å (Table 2), and the question arises as to the coordination number of Mn^{2+} at the M5 site. Gagné and Hawthorne (2020) list the range of observed $^{[6]}Mn^{2+}$-O distances in oxide and oxysalt structures as 1.968–2.798 Å and the range of <$^{[6]}Mn^{2+}$-O> distances as 2.134–2.305 Å; the observed M5-O distances fall within these ranges (Table 2), and hence we consider the M5 polyhedron as an octahedron. The M5 octahedra share edges to form a very unusual trimer (Fig. 3a). Edge-sharing between octahedra is extremely common in oxide and oxysalt structures, and the usual arrangement of a trimer of edge-sharing octahedra is shown in Figure 3b for the M6 octahedra in layer m = 4, in which the shared edges (shown in red in Fig. 3) meet at the center of the trimer. In the M5 trimer (Fig. 3a), the shared edges form the vertical (sub-parallel to **c**) edges of a twisted triangular prism that forms an empty channel through the center of the M5 trimer. The reason for this arrangement is not apparent but may be related to the different stoichiometries of the two arrangements: M5: $[M_3O_{12}]$; M6: $[M_3O_{13}]$. The M5 trimers link into a sheet by sharing corners with tetrahedra; the T2As tetrahedron points in the +**c** direction and the T3As tetrahedron points in the –**c** direction (Fig. 2a). Figure 2b shows the analogous layer in the structure of mcgovernite in which the unit cell is shifted relative to that in dixenite by ⅓ ⅔ in the (001) plane. In mcgovernite, there is only one crystallographically distinct tetrahedron in this layer, and this tetrahedron is occupied by Si. The Z1 tetrahedron in mcgovernite occupies a position similar to the M5 octahedron in dixenite but does not link to other Z1 tetrahedra by sharing vertices; however, the pattern of Z1 tetrahedra in the m = 7 layer in mcgovernite (Fig. 2b) resembles the pattern of M5 polyhedra in the m = 0 layer of dixenite (Fig. 2a).

At m = 1 (Fig. 2c), the layer consists of trimers of edge-sharing M4 octahedra linked by sharing corners with $As^{3+}O_3$ groups. In the topologically analogous layer in mcgovernite (m = 6; Fig. 2d), the trimers of M5 octahedra are linked by SiO_4 groups. In dixenite, the corners of the unit cell are situated at holes in the layer (Fig. 2c). This hole has a very low occupancy by Cu (M2A site; Table 2), and we have denoted the corresponding layer as m = 1′ as it is disordered with the m = 1 layer. In the m = 1′ layer (Fig. 2e) in dixenite, there is an M2A octahedron at the origin of the unit cell that shares edges with the octahedra of the M4 trimers to form an interrupted sheet of octahedra with $As^{3+}O_3$ groups occupying the interstices. A similar layer occurs in mcgovernite (Fig. 2f) except that the $As^{3+}O_3$ groups in dixenite are replaced with SiO_4 groups in mcgovernite.

The m = 2 layer in dixenite (Fig. 2g) consists of isolated $Cu^{+}As^{3+}_4$ groups that link to isolated M1 and M2 octahedra through two distinct $As^{3+}O_3$ groups: As2 and As3. There is no analogous layer in the structure of mcgovernite.

In the m = 3 layer in dixenite (Fig. 2h), trimers of M7 octa-

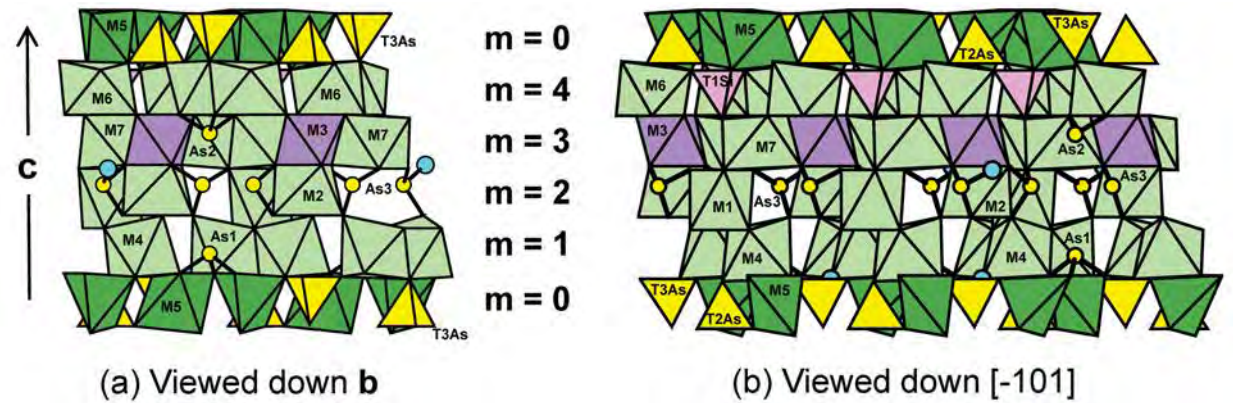

Figure 1. The five unique layers in dixenite (m = 0–4) that stack along the **c**-axis.

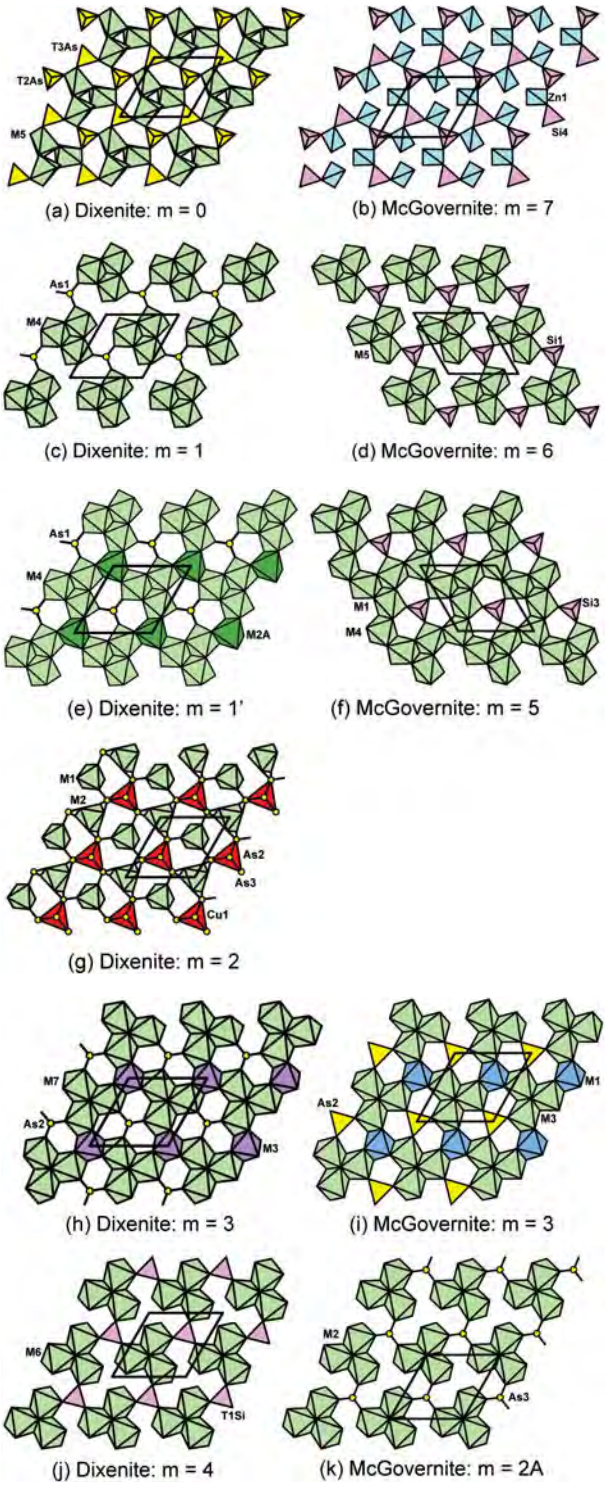

FIGURE 2. Plan views of layers in dixenite compared to similar layers in mcgovernite. Detailed comparisons given in text.

hedra share edges with a single M3 octahedron to form an interrupted sheet in which $As^{3+}O_3$ groups link to the surrounding M7 octahedra. The analogous m = 3 layer in mcgovernite (Fig. 2i) has the same connectivity except that there are $As^{5+}O_4$ tetrahedra

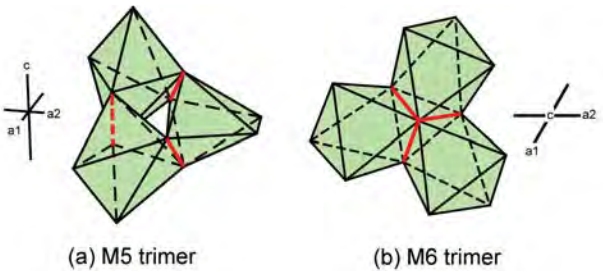

FIGURE 3. The corner-sharing M5 and edge-sharing M6 trimers in dixenite.

in the interstices of the sheet and the M1 octahedron, although dominated by Mn^{2+}, is occupied by a considerable amount of Mg.

The m = 4 layer in dixenite (Fig. 2j) consists of edge-sharing trimers of M6 octahedra linked by sharing corners with SiO_4 tetrahedra; note that this layer differs from the m = 1 layer in dixenite in that the trimers have different orientations (Figs. 2c and 2j). The analogous layer in mcgovernite is m = 2A (Fig. 2k) in which the trimers are linked by $As^{3+}O_3$ groups.

The ($Cu^{+}As^{3+}_{4}$) arrangement

There are two Cu sites, Cu1 and Cu2, that are 0.879(8) Å apart, and hence both cannot be locally occupied. The two sites are jointly coordinated by a trigonal bipyramid of As^{3+} ions (Fig. 4). The refined site-scattering at the two Cu sites, in accord with aggregate occupancy of the two Cu sites, is $Cu^{+}_{0.85} + \square_{0.15}$; at any Cu1-Cu2 pair, one Cu site is occupied by Cu^{+} and the locally associated Cu site is vacant. The neighboring As sites are fully occupied by As^{3+}. Where both sites are locally not occupied, the lone pairs on the locally associated As^{3+} ions will point toward the unoccupied Cu1 and Cu2 sites.

The coordination of each of the Cu sites is illustrated in Figure 4 in which each Cu^{+} ion is [4]-coordinated by As^{3+}. Each coordinating As^{3+} ion bonds to three O atoms at distances of ~1.76 Å and one Cu^{+} ion at distances of 2.34–2.50 Å. The oxygen atoms bonded to As^{3+} are arranged in a trigonal pyramidal arrangement; the range of As^{3+}-O distances (1.73–1.78 Å) are well within the range of 1.67–1.85 Å given by Gagné and Hawthorne (2018) for $^{[3]}As^{3+}$-O distances in all inorganic oxide and oxysalt compounds, and the mean distance of 1.76 Å is close to their grand mean $^{[3]}As^{3+}$-O distance of 1.776 Å. Thus, the Cu^{+} ions are each coordinated by four As^{3+}-O_3 groups in a tetrahedral arrangement. Such As^{3+}-O_3 groups are characterized by a stereoactive lone-pair of electrons extending away from the As^{3+} ion on the side opposing the three O atoms. In the atom arrangements shown in Figure 4, it is apparent that the stereoactive character of the lone electron pair is suppressed by the presence of Cu^{+} as a fourth ligand to As^{3+}: $As^{3+}O_3Cu^{+}$. The Cu1-As distances are 2.400 × 3, 2.342, and 3.378 Å, and the Cu2-As distances are 2.369 × 3, 2.499, and 3.221 Å. It is apparent that Cu1 and Cu2 are each coordinated by four As^{3+} ions, and the longer distances >3.2 Å are not bonded interactions. Inspection of Figure 4 shows that the splitting of Cu into two separate sites, Cu1 and Cu2, is driven by the need for Cu^{+} to shorten the bond to As^{3+}, either As1 or As2, and the 1:1 split suggests that this is not long-range ordered.

Cu^{+}-As^{3+} interactions are not common in crystal structures,

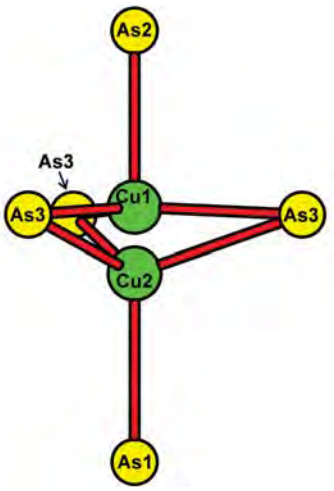

FIGURE 4. Coordination of split Cu1 and Cu2 sites in dixenite.

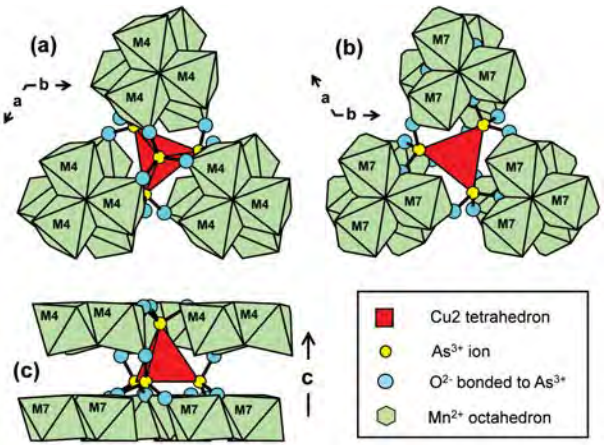

FIGURE 5. Illustration of the incorporation of $[Cu^{+}(As^{3+}O_3)_4]$ clusters into the layered structure.

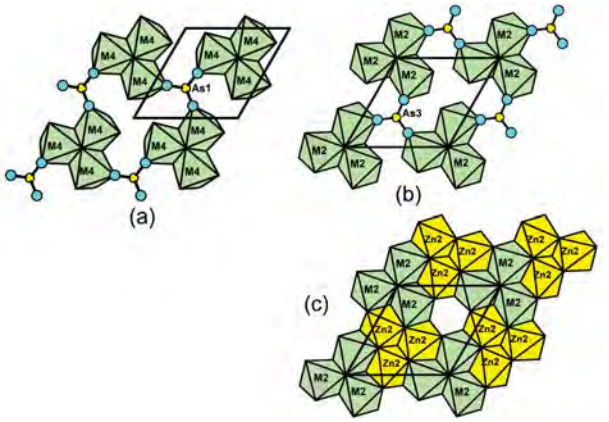

FIGURE 6. Comparison of the M(4)-As(1) layer in dixenite with M(2)-As(3) layer in mcgovernite.

but such bonds have been reported in a few metallo-organic structures. Karagiannidis et al. (1991a) lists a single Cu^{+}-As^{3+} bond of 2.371(1) Å in $[Cu(tclH)_2(AsPh_3)Br]$ in a $(Cu^{+}As^{3+}S_2^{2-}Br^{-})$ tetrahedron, and Karagiannidis et al. (1991b) lists Cu^{+}-As^{3+} distances of 2.411(2) and 2.372(2) Å in $Cu(tclH)(AsPh_3)_2Br$ in a $(Cu^{+}As_2^{3+}S^{2-}Br^{-})$ tetrahedron. The distances are sufficiently similar to those reported for Cu^{+}-As^{3+} in Table 2 to suggest that the atomic arrangements shown in Figure 4 are chemically reasonable.

Fitting the $[Cu^{+}(As^{3+}O_3)_4]$ clusters into the layered structure

The $[Cu^{+}(As^{3+}O_3)_4]$ clusters have quite complicated atom arrangements and it is surprising to encounter them in a close-packed structure. The way in which they are incorporated is illustrated in Figure 5. There is a layer of trimers of Mn^{2+} octahedra (Fig. 5a) in which adjacent trimers provide a triangle of O atoms that link to As^{3+} at the apical position of the $(Cu^{+}As_4^{3+})$ tetrahedron centered at the Cu2 site. Figure 5b shows a view of the same arrangement in the other direction where the linkage of the other $(As^{3+}O_3)$ groups to the underside of the M4 trimers and to the underlying layer of M(7) trimers is apparent. Thus, the two layers of M-trimers are linked by the $[Cu^{+}(As^{3+}O_3)_4]$ cluster involving the Cu^{+} ion at the Cu2 site. As is apparent from Figure 4, the corresponding $[Cu^{+}(As^{3+}O_3)_4]$ cluster involving the Cu1 site points in the opposite direction.

Figure 6 compares the M(4)-As(1) layer in dixenite with the M(2)-As(3) layer in mcgovernite. Both layers consist of trimers of octahedra linked by $(As^{3+}O^{3})$ groups, but the patterns of distribution of the $(As^{3+}O_3)$ groups are complementary. The layer in mcgovernite (Fig. 6b) is disordered with the layer shown in Figure 6c; in that layer the $As^{3+}O_3$ groups are replaced by a trimer of Z(2) octahedra in which the octahedra are only partly occupied. It is striking that the other layers in mcgovernite with the same pattern of trimers and linking (SiO_4) groups (layers m = 4 and m = 6; Hawthorne 2018) do not show this disorder. It is not clear at the moment what is causing the presence of the unusual $[Cu^{+}(As^{3+}O_3)_4]$ cluster in dixenite and the analogous disordered layers of trimers of partly occupied octahedra in mcgovernite. It is to be hoped that a more comprehensive examination of all the basic manganese-silicate-arsenate-arsenite minerals (including two potentially new minerals, work in progress) will allow us to understand why Cu^{+}-As^{3+} bonds form in some of these structures.

IMPLICATIONS

The basic manganese-iron arsenate-arsenite-silicate minerals of the Långban-type deposits in Bergslagen, Sweden, form a family of very complicated layered structures, several of which contain local exotic atomic arrangements embedded within their close-packed structures. Examples are the $[Cu^{+}(As^{3+}O_3)_4]$ cluster and the $[Mn_3^{2+}O_{12}]$ cluster reported here in dixenite and the local replacement of an $As^{3+}O_3$ group by a $[Mg,Mn_3^{2+}O_{13}]$ cluster in mcgovernite and carlfrancisite (Hawthorne 2018). In the same type of deposit, magnussonite (Moore and Araki 1979), although a defect-fluorite structure, contains a $[Mn^{+}As_6^{3+}]$ cluster. The presence of these exotic clusters in densely packed Mn^{2+} octahedra is not understood at the moment but may be related to the relaxation of accumulated strain. There is the potential to incorporate exotic clusters with unusual properties into dense oxide matrices and hence develop materials with desirable physical properties if the

details of their incorporation can be understood. With only two minerals that contain metallic clusters in an oxide matrix, little is known about such clusters and compounds. In both minerals, the semimetal As is an essential component of the cluster, and that class of elements may facilitate their formation in oxide matrices. Metal clusters on two-dimensional substrates are studied extensively in the science of non-volatile memory materials, and the existence of such clusters in three-dimensional mineral structures may provide a template for important industrial materials. The detailed re-examination of dixenite described herein and the discovery and description of increasingly complex mineral structures over the past decade illustrate that minerals provide a rich template for important synthetic materials.

Acknowledgments

Both authors are also grateful for years of interaction with the late Paul Brian Moore and for his suggestion that we look at dixenite more closely. The authors are grateful for the editorial handling of Oliver Tschauner and the detailed reviews of Anthony R. Kampf, Martin Kunz, and the *American Mineralogist* Technical Editor.

Funding

This work was supported by a Discovery grant from the Natural Sciences and Engineering Research Council of Canada and a Canada Foundation for Innovation Grant, both to F.C.H., and by NSF grants EAR-0003201 and MRI 1039436 to J.M.H.

References cited

Araki, T., and Moore, P.B. (1981) Dixenite, $Cu^{1+}Mn^{2+}_{14}Fe^{3+}(OH)_6(As^{3+}O_3)5(As^{5+}O_4)$: Metallic $[As^{3+}_4Cu^{1+}]$ clusters in an oxide matrix. American Mineralogist, 66, 1263–1273.

Bollmark, B. (1999) Some aspects of the origin of the deposit. In D. Holtstam and J. Langhof, Eds., Långban: The Mines, their minerals, geology and explorers, p. 43–49. Raster Förlag, Stockholm, Sweden.

Cooper, M.A., and Hawthorne, F.C. (1999) The effect of differences in coordination on ordering of polyvalent cations in close-packed structures: The crystal structure of arakiite and comparison with hematolite. Canadian Mineralogist, 37, 1471–1482.

——— (2012) The crystal structure of kraisslite, $^{[4]}Zn_3(Mn,Mg)_{25}(Fe^{3+},Al)(As^{3+}O_3)_2[(Si,As^{5+})O_4]_{10}(OH)_{16}$, from the Sterling Hill mine, Ogdensburg, Sussex County, New Jersey, U.S.A. Mineralogical Magazine, 76, 2819–2836.

Gagné, O., and Hawthorne, F.C. (2015) Comprehensive derivation of bond-valence parameters for ion pairs involving oxygen. Acta Crystallographica, B71, 562–578.

——— (2018) Bond-length distributions for ions bonded to oxygen: Metalloids and post-transition metals. Acta Crystallographica, B74, 63–78.

——— (2020) Bond-length distributions for ions bonded to oxygen: Results for the transition metals and quantification of the factors underlying polyhedral distortion via bond-length variation. IUCrJ, 7, 581–629.

Hawthorne, F.C. (2018) Long-range and short-range cation order in the crystal structures of carlfrancisite and mcgovernite. Mineralogical Magazine, 82, 1101–1118.

Hawthorne, F.C., Abdu, Y.A., Ball, N.A., and Pinch, W.W. (2013) Carlfrancisite: $Mn^{2+}_3(Mn^{2+},Mg,Fe^{3+},Al)_{42}[As^{3+}O_3]_2(As^{5+}O_4)_4[(Si,As^{5+})O_4]_6[(As^{5+},Si)O_4]_2(OH)_{42}$, a new arseno-silicate mineral from the Kombat mine, Otavi Valley, Namibia. American Mineralogist, 98, 1693–1696.

Hawthorne, F.C., Kampf, A.R., and Hervig, R. (2019) Memorial of Paul Brian Moore 1940–2019. American Mineralogist, 104, 1062–1063.

Holtstam, D., and Langhof, J., Eds. (1999) Långban, the Mines, their Minerals, History and Explorers, pp. 215. Raster Förlag, Stockholm.

Karagiannidis, P., Akrivos, P.D., Mentzafos, D., and Terzis, A. (1991a) New class of Cu(I) complexes with 2-thioxohexamethyleneimine (tclH) and Group V_A donors. Crystal structure of $[Cu(tclH)_2(AsPh_3)Br]$. Inorganica Chimica Acta, 181, 263–267.

Karagiannidis, P., Akrivos, P., Aubry, A., and Skoulika, S. (1991b) Synthesis and study of mixed ligand monomer Cu(I) compounds with Cu-As bonds. Crystal and molecular structure of bis(triphenylarsine)-(2-thioxohexamethyleneimine) copper(I) bromide. Inorganica Chimica Acta, 188, 79–83.

Lundström, I. (1999) General geology of the Bergslagen ore region. In D. Holtstam and J. Langhof, Eds., Långban: The mines, their minerals, geology and explorers, p. 19–27. Raster Förlag, Stockholm, Sweden.

Moore, P.B. (1970) Mineralogy and chemistry of Långban type deposits in Bergslagen, Sweden. Mineralogical Record, 1, 154–172.

Moore, P.B., and Araki, T. (1979) Magnussonite, manganese arsenite, a fluorite derivative structure. American Mineralogist, 64, 390–401.

Nysten, P., Holtstam, D., and Jonsson, E. (1999) The Långban minerals. In D. Holtstam and J. Langhof, Eds., Långban: The mines, their minerals, geology and explorers, p. 89–183. Raster Förlag, Stockholm, Sweden.

Manuscript received October 16, 2020
Manuscript accepted November 4, 2020
Manuscript handled by Oliver Tschauner

Endnote:

[1]Deposit item AM-21-107719, CIF. Deposit items are free to all readers and found on the MSA website, via the specific issue's Table of Contents (go to http://www.minsocam.org/MSA/AmMin/TOC/2021/Oct2021_data/Oct2021_data.html). The CIF has been peer-reviewed by our Technical Editors.